Life Sciences 211 (2018) 51–62

Contents lists available at ScienceDirect

Life Sciences

journal homepage: www.elsevier.com/locate/lifescie

# The protective effects of acupoint gel embedding on rats with myocardial ischemia-reperfusion injury

Changchun Ji[a,b,c,1], Fan Song[b,d,1], Guoyou Huang[a,b,1], Siwang Wang[d], Han Liu[a,b], Shaobao Liu[a,b], Liping Huang[c], Shaoming Liu[c], Jingyu Zhao[e], Tian Jian Lu[b,f,g,*], Feng Xu[a,b,**]

[a] MOE Key Laboratory of Biomedical Information Engineering, School of Life Science and Technology, Xi'an Jiaotong University, Xi'an 710049, PR China
[b] Bioinspired Engineering and Biomechanics Center (BEBC), Xi'an Jiaotong University, Xi'an 710049, PR China
[c] Department of Acupuncture and Moxibustion, Shaanxi Hospital of Traditional Chinese Medicine, Xi'an 710003, PR China
[d] Department of Chinese Materia Medica and Natural Medicines, School of Pharmacy, Air Force Medical University, Xi'an 710032, PR China
[e] Department of Acupuncture and Moxibustion, Xi'an Hospital of Traditional Chinese Medicine, Xi'an 710021, PR China
[f] State Key Laboratory of Mechanics and Control of Mechanical Structures, Nanjing University of Aeronautics and Astronautics, Nanjing 210016, PR China
[g] MOE Key Laboratory for Multifunctional Materials and Structures, Xi'an Jiaotong University, Xi'an 710049, PR China

ARTICLE INFO

*Keywords:*
Acupuncture
Injectable gel
Cardioprotective effect
Myocardial ischemia-reperfusion injury
*In vivo* microenvironment

ABSTRACT

*Aims:* Prevention and treatment of myocardial ischemia-reperfusion (I/R) injury has for many years been a hot topic in treating ischemic heart disease. As one of the most well-known methods of complementary and alternative medicine, acupuncture has attracted increasing interest in preventing myocardial I/R injury due to its remarkable effectiveness and minimal side effect. However, traditional acupuncture approaches are limited by cumbersome execution, high labor costs and inevitable pain caused by frequent stimulation. Therefore, in this work, we aimed to develop a novel acupoint gel embedding approach and investigated its role in protecting against myocardial I/R injury in rats.

*Main methods:* Gels were embedded at bilateral Neiguan (PC6) points of rats and their protective effects against myocardial I/R injury evaluated in terms of changes in histomorphology, myocardial enzymology, antioxidant capacity, anti-inflammatory response, and anti-apoptosis of cells.

*Key findings:* We found that the approach of acupoint gel embedding could significantly reduce myocardial infarcted size, repair pathological changes, mitigate oxidative stress damage and inflammatory response, as well as inhibit apoptosis of cardiomyocytes. Such cardioprotective effects were found to be associated with Notch-1/Jagged-1 signaling pathway.

*Significance:* The proposed approach of acupoint gel embedding has advantages in continuous acupoint stimulation, dosing controls, and no side effects in the course of treatment, as well as in reducing the pain caused by frequent acupuncture. It can form an alternative therapy to not only protect against myocardial I/R injury but also hold great potential in treating other diseases in the future.

## 1. Introduction

Ischemic heart disease (IHD) is the leading cause of life-threatening diseases and has been a worldwide health problem for many years [1]. The key to successful treatment of IHD is to restore blood supply to the myocardium in time [2]. However, myocardial tissue reperfusion in the ischemic area may generate a large number of reactive oxygen species (ROS) and inflammatory factors and induce over-aggregation of inflammatory cells in the myocardial tissue, which can lead to reperfusion injury and further cause heart damage, arrhythmia and a series of serious clinical consequences [3]. Therefore, prevention and treatment of myocardial ischemia-reperfusion (I/R) injury has been a hot topic in treating IHD [4]. Various approaches have been developed to prevent myocardial I/R injury, such as pharmacological preconditioning [5,6]

* Correspondence to: T. J. Lu, State Key Laboratory of Mechanics and Control of Mechanical Structures, Nanjing University of Aeronautics and Astronautics, Nanjing 210016, PR China.
** Correspondence to: F. Xu, MOE Key Laboratory of Biomedical Information Engineering, School of Life Science and Technology, Xi'an Jiaotong University, Xi'an 710049, PR China.
*E-mail addresses:* tjlu@xjtu.edu.cn (T.J. Lu), fengxu@xjtu.edu.cn (F. Xu).
[1] These authors contributed equally.

https://doi.org/10.1016/j.lfs.2018.09.010
Received 27 April 2018; Received in revised form 4 September 2018; Accepted 4 September 2018
Available online 05 September 2018
0024-3205/ © 2018 Elsevier Inc. All rights reserved.

and acupuncture pretreatment [7]. Among these, acupuncture, one of the most famous complementary and alternative medical therapies that has been applied to treat diseases for > 3000 years [8–10], has attracted increasing interest due to its remarkable effectiveness and minimal side effect [11–13]. However, at present, most reported acupuncture studies employ stainless steel needle, which is limited by cumbersome execution, high labor costs and inevitable pain caused by frequent stimulation [14]. To optimize the way of acupuncture stimulation and improve the special performance of needle tools, much exploration has been attempted [15,16]. For instance, acupoint embedding therapy has been proposed [17,18], with surgical catgut commonly adopted. However, such approach suffers from serious inflammatory response and limited control over the chemophysical properties of surgical catgut that are associated with acupoint stimulation ability. Therefore, there is still an unmet need for new approaches to facilitate the development and applications of acupuncture pretreatment in preventing myocardial I/R injury.

Recently, injectable gels have emerged as attractive embedding materials, enjoying widespread biomedical applications [19,20]. While injectable gels can maintain liquid sol form before injection, they rapidly transit to solid gel form at physiological environment after injection, thus ideal for *in vivo* application since they can be used in a minimal invasive manner. Moreover, the chemophysical properties of injectable gels can be easily adjusted to fulfill specific requirements for maximizing their outcomes. To date, numerous injectable gels, including biodegradable polymers (*e.g.*, poly(glycolic acid) (PGA), poly (lactic acid) (PLA), polycaprolactone (PCL) and poly(lactic-*co*-glycolic acid) (PLGA)) and hydrogels (*e.g.*, collagen, gelatin, alginate and chitosan, as well as their derivatives) have been developed and widely used as carriers for delivering therapeutic agents or as *in situ* forming three-dimensional (3D) scaffolds for supporting the ingrowth of cells and the deposition of new extracellular matrix (ECM) [20–22]. However, the use of these injectable gels for acupoint embedding therapy in preventing myocardial I/R injury is not yet explored.

In this work, we investigated the protective effects of acupoint gel embedding against myocardial I/R injury in rats (Fig. 1). As for acupoint stimulation, the degradation rate and mechanical properties of gels are quite important in addition to biocompatibility. Among the US Food and Drug Administration (FDA)-approved degradable polymers, PLGA, as a type of copolymers of PGA and PLA, can be readily tuned with well-controlled degradation rates and mechanical properties by integrating the advantages of both PGA and PLA [23]. In addition, PLGA dissolved in *N*-methy-2-pyrrolidinone can form insoluble PLGA gels rapidly at mild body conditions after injection, making it well-suited to be used as acupoint injectable gel [24]. Therefore, we used PLGA as the injectable gel. As for acupoints, it has been well established that the Neiguan (PC6) points play important roles in treating cardiovascular diseases, *e.g.*, prevention and treatment of myocardial I/R injury [25–28]. We used the injected PLGA gels to stimulate the PC6 points of rats and explored the protective effects from various aspects, including myocardial lesion area, histomorphology, myocardial enzymology, antioxidant capacity, anti-inflammatory effects, and anti-apoptosis of cells. The mechanism underlying the protective effects was discussed. This acupoint gel embedding method can not only become an alternative approach of traditional acupuncture to reduce myocardial I/R injury, but also provide a platform to develop new therapies that integrate modern technologies with Traditional Chinese Medicine.

## 2. Materials and methods

### 2.1. Animals

Male Sprague-Dawley (SD) rats (220 ± 20 g) were purchased from the Experimental Animal Research Center of the Fourth Military Medical University, Xi'an, China. The animals were maintained in a temperature controlled room (20.1–23.1 °C; 40–50% humidity), under a 12-h:12-h light–dark cycle, with free access to water. All the experimental protocols were approved by the Laboratory Animal Administration Committee of Xi'an Jiaotong University and performed according to the Guidelines for Animal Experimentation of Xi'an Jiaotong University.

### 2.2. Injectable gel preparation

PLGA (Shandong Province Medical Devices Research Institute, Jinan, China) was crushed into fine flour and mixed with *N*-methy-2-pyrrolidinone (Nanjing SPC Scientific Co. Ltd., Nanjing, China) and poly(ethylene glycol) 400 (Aladdin Industrial Inc., Shanghai, China) at the mass ratio of 25:65:10. The mixture was vortexed at room temperature for 1 h to completely dissolve PLGA. The dissolved solution of PLGA was then stored at room temperature and protected from light before using.

### 2.3. Acupoint gel embedding

Acupoints positioning in SD rats were referenced to internationally recognized standards, *i.e.*, the China Acupuncture Society of Experimental Acupuncture Branch to develop the “animal moxibustion acupuncture points map.” Rat PC6 point located in the front of the two forelimbs is designated the point at 1/6 of the anterior forearm length above the rasceta between the ulna and the radius [29]. A micro-injection pump was used to quantitatively inject 10 μL dissolved solution of PLGA into each rat PC6 point at a rate of 2 μL/s. After injection, the solvent in PLGA solution was quickly replaced by surrounding interstitial fluid, leading to the formation of insoluble PLGA gel form.

### 2.4. Gel characterization

To characterize gel mechanical property, the PLGA gel balls were compressed by Bose biomechanical testing machine (BOSE ELF 3220, ElectroForce System Group, Minnesota, USA). Flat head was used to loading the PLGA gel ball under the displacement control of 2 mm, with a fixed loading rate of 0.1 mm/s. PLGA gel balls in PBS solution at 37 °C were tested respectively, and the displacement-load curve was obtained. Secondly, we developed a finite element (FE) model to simulate the testing process of PLGA gel balls having different Young's moduli but constant Poisson ratio (0.33). The diameters of the PLGA gel balls were measured and the average value of the measurement was 4.4 mm. The loading plate was assumed rigid, and the contact with the loaded ball was non-friction hard contact. The geometric model was axisymmetric, and the element type was CAX4R with the size of 0.2 mm.

To quantify and predict the mechanical stimulation intensity to the acupoint, the injection of gel ball into the tissue was modeled as indentation in an infinite body. An axisymmetric FE model was developed to simulate such indentation. The geometry was meshed with triangle elements with the size of 0.2 mm for the gel ball and near the region of contact, but the other part with the size of 0.4 mm (Supplementary Fig. 1A). The stress along the direction of indentation is presented in Supplementary Fig. 1B. The Young's modulus of tissue was set at 0.01 MPa. We present the strain energy of the model for different Young's moduli (0.01–100 MPa) and diameters ($d$ = 2–5 mm) of gel ball. To characterize *in vivo* gel degradation, the embedded PLGA gels were taken out per week and their dry weights were measured.

### 2.5. Rat myocardial I/R model

The model was established following our previous study [30–32]. We choose to ligating the left anterior descending (LAD) coronary artery by utilizing polypropylene suture to establish an ischemic model, monitored by electrocardiogram (ECG, BL-420S Biological Function Experiment System, Chengdu Thaimeng Technology Co. Ltd., Shanghai, China). MI model success is based on the change of ECG: A few minutes

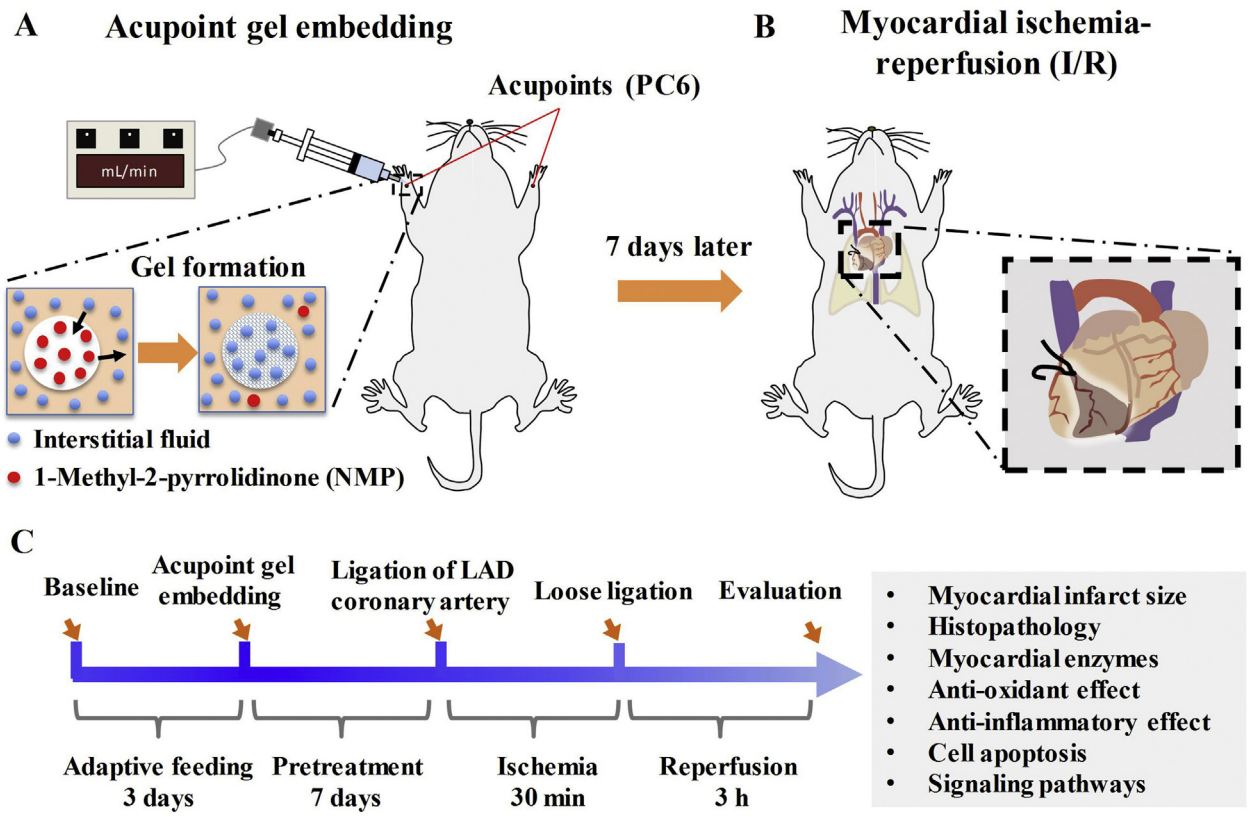


**Fig. 1.** Schematics on acupoint gel embedding for preventing myocardial I/R injury in rats. (A) A microinjection pump is used to quantitatively inject dissolved solution of PLGA into each PC6 point of rats. After injection, the solvent in PLGA solution is quickly replaced by surrounding interstitial fluid, leading to the formation of insoluble PLGA gel form. (B) After 7 days' treatment, myocardial ischemia is induced by ligating the left anterior descending (LAD) coronary artery 2 mm from the tip of the left auricle, utilizing polypropylene suture. After 30 min of ischemia, the slipknot is released, and the myocardium is reperfused for 3 h. In the control group, rats are subjected to surgery using the same protocol, except that the coronary artery is not ligated. (C) Experimental progress of the timeline and the main evaluation indicators.

after the onset of an acute myocardial infarction (AMI), a short-term subendocardial ischemic insult was initiated, resulting in an abnormally high T-wave on the ECG, followed by an upward ST-segment elevation or arch-back elevation, connected to the upright T wave. In addition, the amplitude of QRS increased and slightly widened with/without abnormal Q wave. Therefore, ST segment elevation is the main criterion for judging the early stage of AMI (Supplementary Fig. 2). After 30 min of ischemia, the ligature line was open and the myocardium was re-perfused for 3 h. In the control group, ten rats were through LAD, but not ligated. Different groups received different treatments.

### 2.6. Experimental groups

Rats were randomly divided into four groups ($n = 10$): (I) **CON**: Rats received no acupuncture pre-stimulation, and were through LAD, but not ligated; (II) **I/R**: Rats received no acupuncture pre-stimulation, but were constructed by LAD ligation for 30 min, and then the LAD was allowed 3 h reperfusion; (III) **PC6 + CON**: Rats received acupuncture pre-stimulation at PC6 points (7 days before I/R operation), but not ligated; (IV) **PC6 + I/R**: Rats received acupuncture pre-stimulation at PC6 points (7 days before I/R operation), and were constructed by LAD ligation for 30 min, followed by 3 h reperfusion of LAD.

### 2.7. Determination of myocardial infarct size

After 3 h for reperfusion, we re-occluded the LAD artery. Upon reversing the infused Evans blue (1%) *via* aorta, the non-ischemic area was turning to blue but the area at risk (AAR) was not. After frozen at −20 °C for 2–3 h, the heart was cut into six transverse slices (2 mm for each) from apex to base. The slices were then allowed to react with 1% triphenylterazolium chloride (TTC) for 15 min at 37 °C, finally fixed in 4% paraformaldehyde. After Evans blue/TTC staining, images of the heart slices were measured *via* ImageJ software. Evans blue staining was used to determine the consistency of ligation sites. TTC staining enables marking the viable tissue in the AAR, which can react with dehydrogenase and turn tissue into red, while the ischemic tissue usually shows decreased dehydrogenase activity and therefore cannot react with Evans blue/TTC, thus showing pale color. The infarct area was represented as a percentage.

### 2.8. Histopathological changes of left ventricular specimens

Heart cavity was rinsed rapidly with cold phosphate buffer saline (PBS) when the rat was sacrificed, with 10% formalin solution used for fixing. Paraffin sections (5 μm sections, Leica RM 2125, Germany) were collected from the left ventricle (LV), and then stained with hematoxylin and eosin (H&E) and examined by light microscopy (Nikon, Tokyo, Japan) at 200× magnification.

### 2.9. Serological detection of secreted proteins and cytokines

All rats were drugged at the end of the experiment. We collected blood (3 mL) from the abdominal aorta. After centrifugation, serum was taken for determining the concentrations of creatine kinase (CK), creatine kinase-MB (CK-MB), lactate dehydrogenase (LDH) and aspartate aminotransferase (AST), anti-oxidation capacity of malonaldehyde (MDA), superoxide dismutase (SOD) and glutathione peroxidase (GSH-PX). The activity of NO was evaluated by using the nitrate reduction

method, which sums the total amount of nitric oxide (NOx), like nitrate ($NO_3^-$) and nitrite ($NO_2^-$). All kits were purchased from Nanjing JianCheng Biological Engineering Research Institute, Nanjing, China. The measurement was performed by using an RT-9600 Semi-automatic Biochemical Analyzer (ShenZhen LeiDu Life Sciences, LLC, Guangxi, Nanning, China). Tumor necrosis factor-α (TNF-α) and interleukin-6 (IL-6) activities were measured by enzyme linked immunosorbent assay (ELISA, Wuhan Boshide Biological Technology Company, Wuhan, China).

### 2.10. Determination of apoptosis

Tissue paraffin section for terminal deoxynucleotidyl transferase-mediated dUTP nick end labeling (TUNEL) assay (situ cell death detection kit, Roche Molecular Biochemicals, Mannheim, Germany) [33]. The index of apoptosis refers to the ratio of the number of apoptotic myocytes to the total number of myocytes counted × 100%.

### 2.11. Western-blotting assays of left ventricular specimens

Expressions of caspase-3, cleaved caspase-3 (c-caspase-3), Bax, Bcl-2, Notch-1 and Jagged-1 were measured using Western blot as described previously [30,33]. Equal amounts (30 μg) of heart tissue from the left ventricular myocardium were homogenized in RIPA lysis buffer at 4 °C for 5 min to get 10% homogenates. After protein quantification, proteins were loaded and separated by sodium dodecyl sulfate polyacrylamide gel electrophoresis (SDS-PAGE). The membranes were blocked by Tris-buffered saline/Tween 20 (TBS-T) containing 5% BSA, then incubated with the primary antibodies: caspase-3, c-caspase-3, Bax, Bcl-2 (1:1000 Santa Cruz Biotechnology, USA), Notch-1, Jagged-1 (1:1000, Cell Signaling, Danvers, MA, USA), and glyceraldehyde 3-phosphate dehydrogenase (GAPDH) (1:1000, Abcam, Cambridge, UK) for 12 h at 4 °C. After repeated washing, the membranes were incubated with horseradish peroxidase-conjugated secondary antibodies (Santa Cruz Biotechnology, Santa Cruz, CA) at a dilution of 1:5000 for 2 h at room temperature. Finally, proteins were visualized using an enhanced chemiluminescence detection system (ECL, Amersham, Buckinghamshire, UK). Quantity One (BioRad, Hercules, CA, USA) was used to carry out densitometry analysis on protein bands of interest.

### 2.12. Statistical analyses

Statistical analyses were performed with analysis software SPSS 21.0 (IBM Corp., Armonk, NY, USA). All data were presented in the form of mean ± SD. Comparisons among more than two experimental groups were determined by two-way ANOVA. Statistical significance between two groups was evaluated with LSD-*t*-test. Significant differences were indicated by $^*P < 0.05$ or $^{**}P < 0.01$.

## 3. Results

### 3.1. Evaluation of degradation and mechanical properties of PLGA gels

Since the intensity of acupoint stimulation is associated with the size and stiffness of the embedded gels, both of which closely related to gel degradation, we anticipated that it could be easy to estimate the intensity from gel degradation kinetics. The embedded PLGA gels in rats were found to degrade almost linearly with time, with nearly 62% original mass remaining post 1 week and 15% remaining post 4 weeks (Fig. 2A). The size of PLGA gel balls (~4 mm) is too small to compress directly by using a regular shape of PLGA gel. Therefore, we compressed the PLGA gel ball directly and then inversely calculated the Young's modulus based on the force-displacement curve. To measure the Young's modulus of PLGA gel balls, the FE method was used to model the process of mechanical testing above. The displacement-load curve was used to simulate PLGA gel balls having different Young's moduli (Fig. 2B). The von Mises stress in a 200 MPa gel ball is presented in Supplementary Fig. 3. In the small deformation regime, it was found that the displacement-load curve obtained in the experiment fell within the range of the simulated displacement-load curve for Young's modulus varying between 100 MPa and 200 MPa. Therefore, we estimated that the Young's modulus range of PLGA gel balls is 100–200 MPa.

To quantify and predict the intensity of mechanical stimulation to the acupoint, the injection of gel balls into the tissue was modeled as an indentation in an infinite body (Supplementary Fig. 1A). With the Young's modulus of tissue given by 0.01 MPa (typical for muscle and skin tissues), we presented the strain energy of the model for different Young's moduli (0.01–100 MPa) and diameters (d = 2–5 mm) of gel balls (Fig. 2C). The results showed that the stimulation intensity increases with both the Young's modulus and diameter of the injected gel balls, indicating that the mechanical stimulation intensity to the acupoint decreases with the degradation of PLGA gels. It is thus effective to control the intensity and duration of mechanical stimulation through tuning the initial properties (*e.g.*, size and Young's modulus) and degradation of injected gels.

### 3.2. Acupoint gel embedding reduced the myocardial infarcted size

Since infarct size is a typical feature of myocardial I/R injury, we characterized the effect of acupoint gel embedding on the myocardial infarcted size using Evans blue/TTC staining (Fig. 3). Evans blue is a kind of high affinity of dyes in blood and plasma albumin and the colored area indicates non-ischemia anoxic area. TTC staining can react with the succinate dehydrogenase of mitochondria in living cells, then turn the tissue to red, which is used to indicate the cell's vitality. In our study, the red areas were referred to as area at risk (AAR). The proportion of left ventricle (LV) area occupied by AAR was used to express the consistency of ligation sites in each experimental group. As results, there is no statistical difference between the groups (Fig. 3A). The I/R group showed a large TTC-negative area (pale), which was the infarcted myocardium (INF) area. But the INF of PC6 + I/R group was obviously smaller than the I/R group and closer to the CON + I/R group. To further analyze the effect, we quantified the area of INF as a percentage of the AAR (INF/AAR) and found that INF/AAR was significantly higher in the I/R group (41.7 ± 7.2%) compared with the PC6 + I/R group (20.9 ± 6.4%) (Fig. 3B). These results indicated that acupoint gel embedding could reduce I/R-induced myocardial infarction.

### 3.3. Acupoint gel embedding remitted pathological changes in myocardial tissue

Since inflammation induces infiltration of inflammatory cells in muscle fibers, causing vascular occlusion and ischemia in severe cases [34], we characterized the effect of acupoint gel embedding on pathological changes in myocardial tissue sections using light microscopy (Fig. 4). We observed that normal myocardial tissue has clear transverse striations, with no cell swelling and structure distortion, and no inflammatory cell infiltration in both the CON and the PC6 + CON groups (Fig. 4A and C). In contrast, we observed obvious amount of myocardial cell swelling, break and degeneration of striated muscles, and numerous infiltrating inflammatory cells in the untreated I/R group (Fig. 4B). However, tissue from the PC6 + I/R group exhibited almost normal myocardial tissue histology, possessing an area of normal myocardial arrangement, clear striated muscles, and fewer massive inflammatory cells infiltrated in Fig. 4D than the I/R group. These results indicated that acupoint gel embedding could remit pathological changes in myocardial tissue.

### 3.4. Acupoint gel embedding reduced the activities of diagnostic marker enzymes

Increase of cell membrane permeability and myocardial ischemic

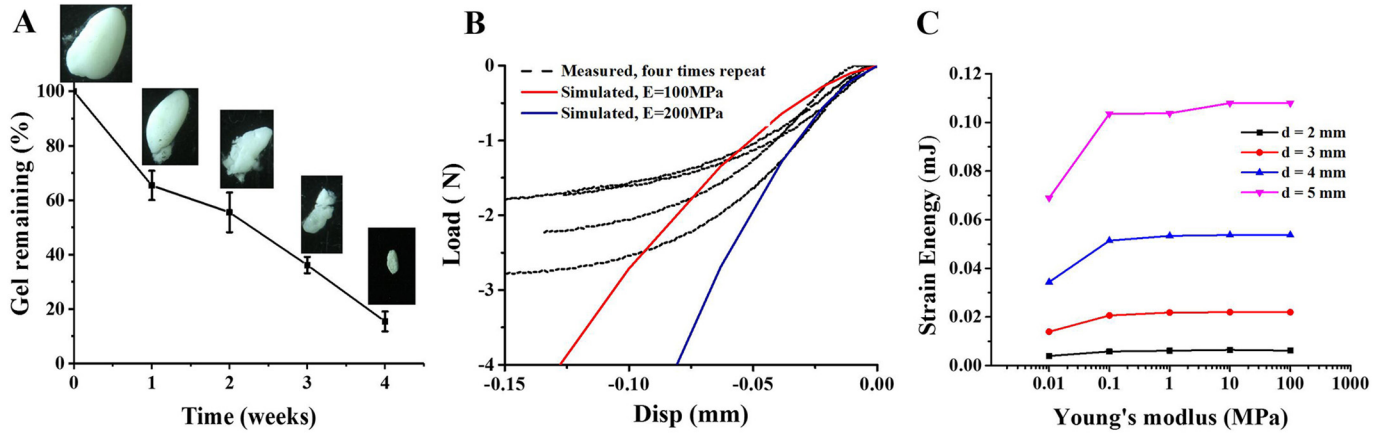


**Fig. 2.** Gel degradation and mechanical properties. (A) The embedded PLGA gels in rats were found to degrade almost linearly with time, with nearly 62% original mass remaining post 1 week and 15% remaining post 4 weeks; (B) measured and simulated load *vs.* displacement curves when compressing a PLGA gel ball within two planes; (C) the injection of PLGA gel into the tissue is modeled as the indentation of a PLGA gel ball into an infinite body. The strain energy of the model for different Young's modulus (0.01–100 MPa) and the diameter ($d$ = 2–5 mm) of PLGA gel ball. Data are shown as mean ± SD, $n$ = 6.

necrosis usually causes various enzymes released into the blood after the occurrence of I/R, and thus variation of serum enzyme concentrations are commonly used to reflect the severity of cardiomyopathy [26,35–38]. Therefore, we characterized the activities of following enzymes: AST, CK, CK-MB and LDH, in different group. As results, a significant increase in these enzyme activities in the serum of I/R group rats was observed (Fig. 5). However, we did not observe any significant difference between the CON and PC6 + CON groups, but the activities of all serum diagnostic marker enzymes in the CON and the PC6 + I/R groups significantly decreased compared to the untreated I/R group. The results indicated that the acupoint gel embedding could maintain the integrity of the cell membrane, internal and external osmotic pressure and regulate cell membrane permeability, thereby limiting the leakage of these indicative enzymes.

### 3.5. Acupoint gel embedding attenuated oxidative stress of I/R rats in the serum

GSH-Px and SOD are antioxidants produced by the body's own system for counteracting ROS abnormalities [39,40]. MDA is a type of lipid peroxidation product that is a key factor for maintaining the fluidity and permeability of cell membranes, and determining the changes in cell structure and function. It is an important indicator for resisting the ROS abnormalities and maintaining the physiological balance of the cells [41]. To further investigate the antioxidant effect of acupoint gel embedding, serum active expression of SOD, MDA and GHS-PX was tested (Fig. 6A–C). We observed that the SOD and GSH-PX activities in the untreated I/R group decreased significantly compared with those in the CON group. Pretreatment at PC6 points increased the activities compared with the I/R group rats (Fig. 6A,C). Compared with the CON group, the activity of MDA in I/R group increased significantly. Pretreatment at PC6 points (PC6 + I/R, PC6 + CON) decreased MDA activity compared with the I/R group rats (Fig. 6B). The results clearly indicated that acupoint gel embedding treatment could reduce I/R oxidative stress by decreasing the activity expressions of MDA, and increasing the activity expressions of SOD and GSH-PX.

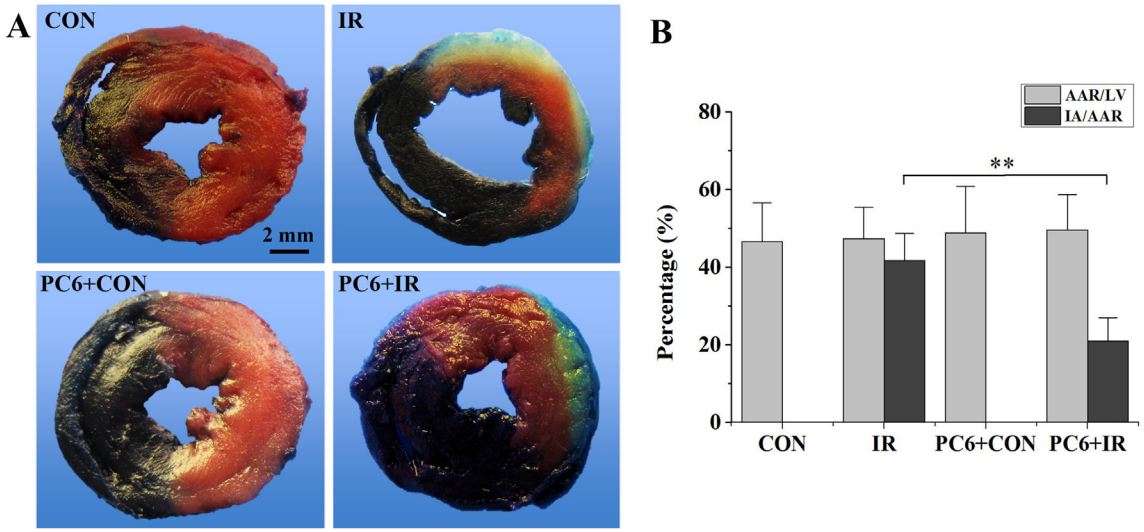


**Fig. 3.** Acupoint gel embedding reduced the myocardial infarcted size. (A) Myocardial infarct size was measured with Evans blue/TTC staining. The blue area represents the remote area, the area at risk (AAR) is stained red and the infarcted size (INF) is pale (the tissue slices were cut from the same location of the heart). (B) The AAR was quantified as a percentage of the total left ventricle (LV; AAR/LV) and INF as a percentage of the AAR (INF/AAR). Data are shown as mean ± SD, $n$ = 3, $^{**}P < 0.01$. (For interpretation of the references to color in this figure legend, the reader is referred to the web version of this article.)

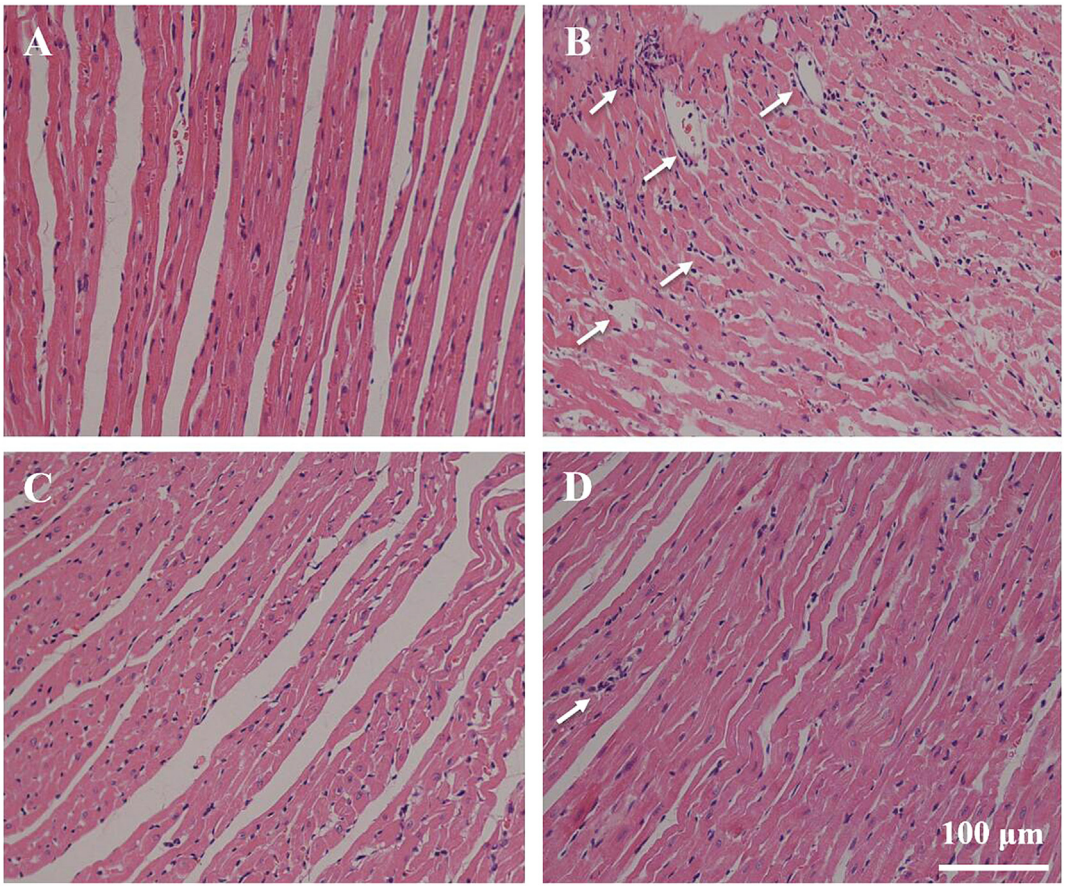


**Fig. 4.** Acupoint gel embedding remitted pathological changes in myocardial tissue. (A) The CON group showed normal myocardial histology, clear transverse striations, and no inflammatory cell infiltration. (B) The I/R group showed swelling of obvious myocardial cells, degeneration, loss of transverse striations, and large numbers of invasive inflammatory cells. (C) The PC6 + CON group showed normal myocardial histology, clear transverse striations, and no inflammatory cell infiltration. (D) The PC6 + I/R group showed an area of normal myocardial arrangement, clear transverse striations, and few invasive inflammatory cells, as indicated by the arrows.

### *3.6. Acupoint gel embedding attenuated inflammatory response in I/R hearts*

To investigate the effect of acupoint gel embedding on inflammatory response in I/R hearts, we characterized the activities of serum TNF-α and IL-6 and observed that they increased significantly in the I/R group compared with those in the CON group (Fig. 7A,B). However, the serum TNF-α and IL-6 activities decreased in the PC6 + I/R group compared with those in the untreated I/R group rats. Due to the active chemical nature of NO, it quickly metabolizes to nitrite and nitrate (NOx) in the body, and nitrite is further converted to nitrate. Thus, the total amount of NOx can be used to evaluate the NO level. We found that the occurrence of I/R causes a dramatic down-regulation of NOx level (Fig. 7C). After acupoint gel embedding treatment, the NOx level is significantly up-regulated and there is a significant difference between the NG + I/R group and the I/R group. These results indicated that acupoint gel embedding could attenuate inflammatory response in I/R hearts.

### *3.7. Acupoint gel embedding inhibited cell apoptosis in myocardial tissue*

To investigate the effect of acupoint gel embedding on cell apoptosis in myocardial tissue, we did TUNEL staining. Apoptotic nuclei were labeled by TUNEL staining (red) while all cell nuclei were labeled by DAPI (blue) (Fig. 8A). We observed a significant increase of apoptotic nuclei in the I/R group compared to that in the CON group, and a reduction in the percentage of TUNEL-positive cells in the PC6 + CON group (Fig. 8B). To study the anti-apoptotic ability of acupoint gel embedding at the molecular level, we also investigated the protein expression of apoptosis signaling molecules, including Bax, Bcl-2, caspase-3, and c-caspase-3 in myocardial tissue (Fig. 9). We observed that, compared with the I/R group, the expression of caspase-3, c-caspase-3 and Bax in other groups all decreased, but the expression of Bcl-2 increased. We also found significant difference in the expression of these proteins between the PC6 + I/R group and the I/R group. The results indicated that administration of I/R produced death of cardiomyocytes in the heart by inducing apoptosis, while acupoint gel embedding could reduce cell apoptosis induced by I/R injury.

### *3.8. Cardioprotective effect of acupoint gel embedding is associated with enhanced Notch-1 signaling*

To investigate the potential mechanisms underlying the cardioprotective effect induced by acupoint gel embedding, the protein levels of Notch-1 and Jagged-1 in myocardial tissues were evaluated by Western blotting analysis (Fig. 10). Compared with the I/R group, the expression levels of Notch-1 and Jagged-1 both increase in the PC6 + CON and PC6 + I/R groups. We observed prominent differences between the I/R group and the PC6 + I/R group, as well as between the CON group and the PC6 + CON group.

## 4. Discussion

Long-time ischemia can cause myocardial tissue necrosis, leading to

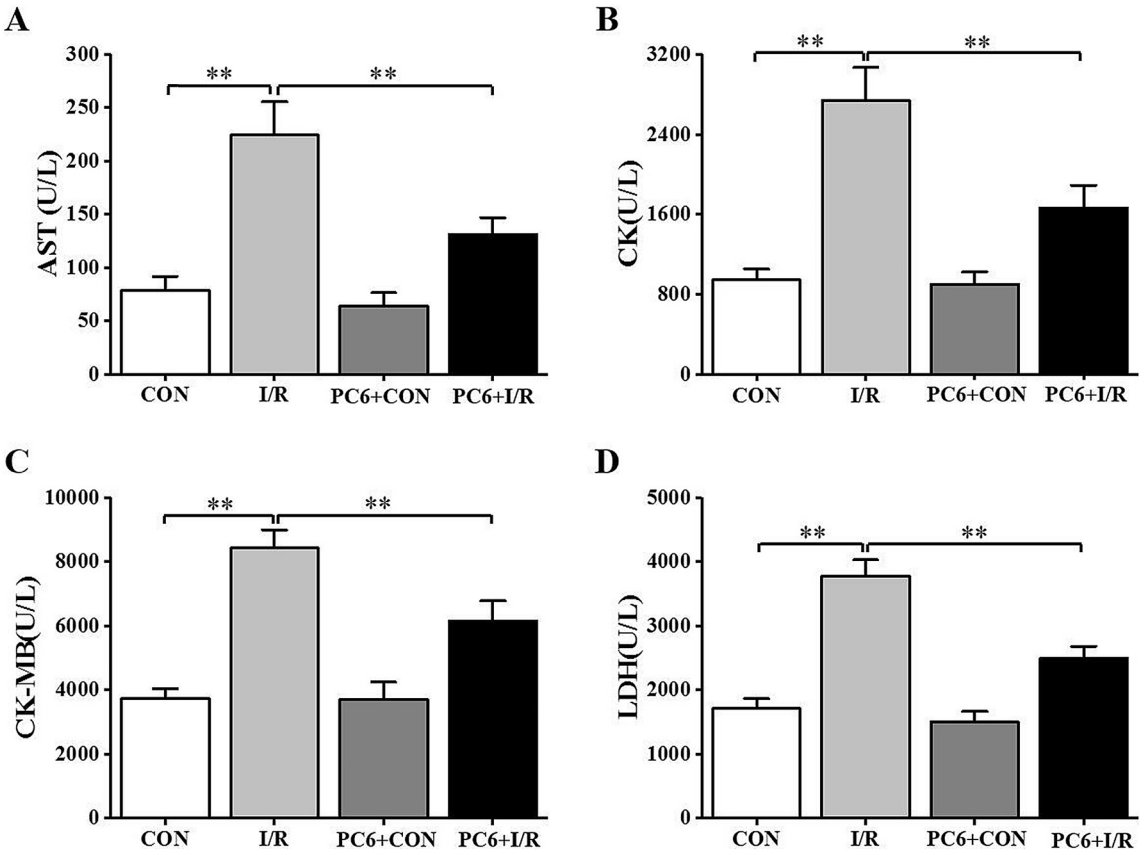


**Fig. 5.** Acupoint gel embedding reduced the activities of diagnostic marker enzymes. (A) The activity expressions of AST. (B) The activity expressions of CK. (C) The activity expression of CK-MB. (D) The activity expressions of LDH. Data are shown as mean ± SD, $n = 10$, $^{**}P < 0.01$.

decreased heart function. For treatment purpose, it is key to timely and effectively recover blood perfusion (*i.e.*, reperfusion), which however often induces secondary and aggravate myocardial tissue injury (*i.e.*, I/R injury). Therefore, it is necessary to use protective drugs or therapeutic means at the beginning of reperfusion to reduce the I/R injury. This treatment idea is consistent with the theory of "treating before illness" in traditional Chinese medicine (TCM). "Treating before illness" is the basic principle of prevention and treatment of diseases by TCM, and "preventive acupuncture" is one of the most important pretreatment measures. As one of the most well-known complementary and alternative medical approach, acupuncture has attracted increasing interest in treating many diseases in modern world due to its minimal side effect.

Various materials and corresponding approaches have been developed to stimulate acupoints, including widely used needle-based acupuncture, moxibustion, electro-acupuncture and acupoint catgut embedding [16,42,43]. Although effective, these approaches either suffer from short-term stimulation, cumbersome to perform and long-term pain, or involve the issues of serious inflammatory response and limited stimulation control [14]. The acupoint gel embedding approach we developed here may address these issues. A significant advantage of acupoint gel embedding is that the degradation rate, the mechanical properties and the volume of the embedded gels can be easily adjusted by choosing the type, the concentration and the injected amount of the injectable materials [44,45]. Therefore, the duration and strength of acupoint stimulus can be easily controlled according to specific requirement. Another advantage of acupoint gel embedding is that it is readily to incorporate other materials into injectable gels to achieve multi-mode stimulation. For example, heat producing nanoparticles can be employed to generate heat at local acupoints to achieve thermal

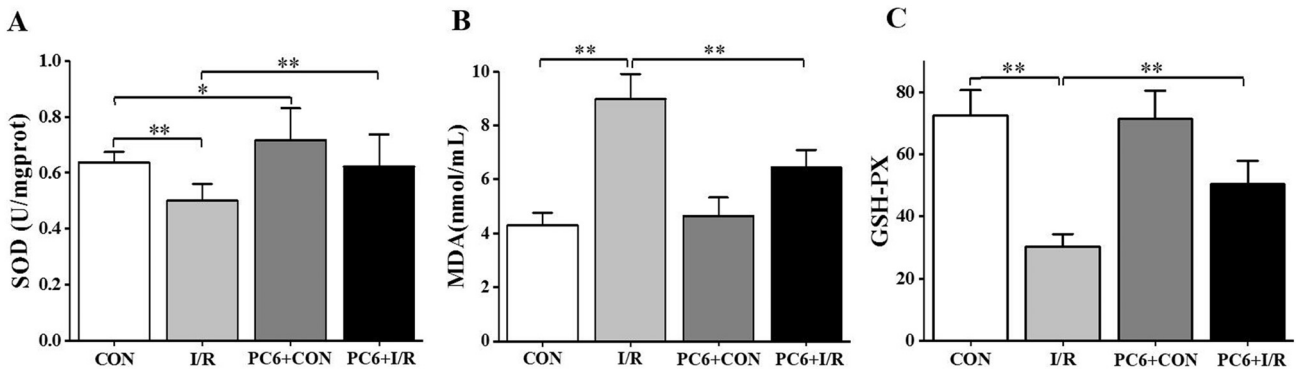


**Fig. 6.** Acupoint gel embedding attenuated oxidative stress in the serum. (A) The activity expressions of SOD. (B) The activity expressions of MDA. (C) The activity expressions of GSH-PX. Data are shown as mean ± SD, $n = 10$, $^{*}P < 0.05$, $^{**}P < 0.01$.

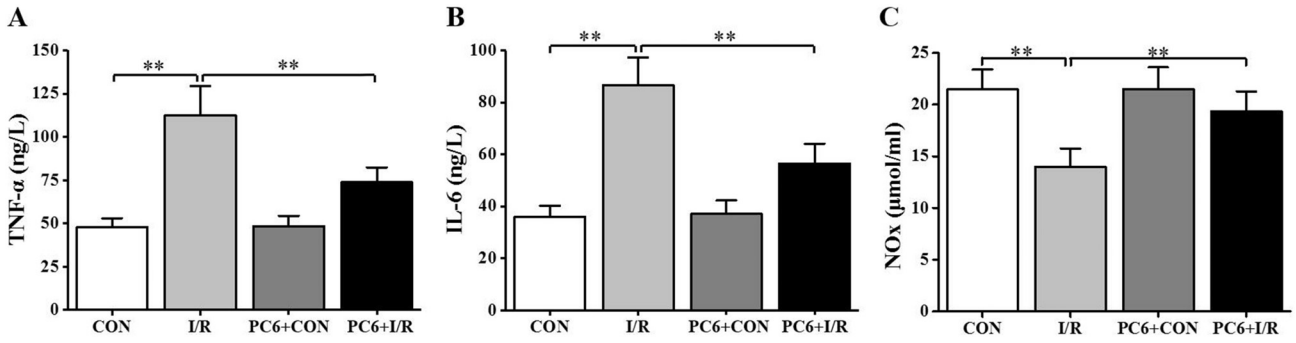


**Fig. 7.** Acupoint gel embedding attenuated inflammatory response in I/R hearts. (A) The activity expressions of TNF-α. (B) The activity expressions of IL-6. (C) The activity expressions of NOx. Data are shown as mean ± SD, $n = 10$, $^{**}P < 0.01$.

stimulation as experienced in moxibustion. In addition, magnetic nanoparticles can be used to apply active mechanical stimulation by generating forces under non-uniform magnetic field [46–48]. Moreover, drugs can be incorporated to provide additional benefits by controlling their delivery and release at acupoints with injectable gels [20,49].

Myocardial injury caused by I/R is often accompanied by changes in myocardial enzymes and cardiac function, causing the appearance of inflammatory reactions, oxidative stress damage, and myocardial apoptosis. In our study, the diagnostic and detection techniques commonly used in western medicine were combined to evaluate the effects of acupoint gel embedding pretreatment on reducing myocardial damage after I/R injury. The heart is known to be one of the most active organs in humans. It contains a large number of enzymes. When the myocardium is damaged by ischemia, the permeability of the cell membrane increases, and the protease in the myocardium is released into the blood. Among them, the detection of AST, CKMB and LDH contents in serum is a commonly used diagnosis method in clinic [50]. In our study, we observed that acupoint gel embedding at PC6 points reduced the activities of AST, CKMB and LDH enzymes caused by I/R, which means the acupoint gel embedding can maintain the integrity and permeability of the structure and function of the heart membrane, thereby limiting the leakage of myocardial enzymes.

IL-6 is the major cytokine involved in the inflammatory response during the immune response. TNF-α is a monocyte factor that is mainly produced by activated mononuclear macrophages. They are not only a primary proinflammatory mediator, but also an important initiation factor that stimulates the cascade effect of inflammation *in vivo* [51–53]. NO is an important component of the relaxing factor secreted by vascular endothelial cells, which has the functions of relaxing blood vessels, inhibiting platelet aggregation and blood cell aggregation and adhesion [54–56]. Because of coronary artery spasm and infarction caused by ischemia and hypoxia, NO synthesis and secretion of vascular endothelial cells drastically decreased, resulting in the oxidation of low density lipoprotein (oxidation low density lipoprotein, ox-LDL); Then leading to endothelial cell dysfunction and promoted inflammatory cell infiltration; Finally, resulting in the further development of atherosclerotic plaque and increased myocardial ischemia [57,58]. Therefore, NO is closely related to the production of inflammation. In our study, acupoint gel embedding limited the release of related inflammatory factors (IL-6, TNF-α), recovered NO release to relieve atheromatous plaque formation and reduce ischemia, predicting its anti-inflammatory response. By explaining from another aspect, acupoint gel embedding plays a prominent role in maintaining the integrity of tissue morphology, reducing inflammatory cell infiltration, and repairing cell pathological changes such as swelling and degeneration.

Myocardial I/R injury can enhance oxidative stress during the acute reperfusion phase [59–61] by increasing the activities of superoxide anion, hydrogen peroxide, and hydroxyl radical [62]. In our research, SOD and GSH-Px are antioxidizes, which are greatly reduced by I/R injury, causing decline in myocardial function. The higher their activities are, the stronger the ability to scavenge free radicals. Therefore, their increased level of activity in the PC6 + I/R group reflects the ability of the acupoint gel embedding to scavenge free radicals. MDA is a product of lipid peroxidation, which affects the fluidity and permeability of cell membrane and ultimately leads to changes in cell structure and function. Therefore, the level of MDA further confirms that acupoint gel embedding has strong resistance to oxidative stress.

Existing studies have shown that the cardiomyocyte apoptosis is a main pathological feature of myocardial I/R injury [38,63,64]. In our research, we first confirmed that acupoint gel embedding effectively reduced the rate of apoptosis and the expression of apoptosis-related proteins (C-caspase 3, caspase 3, Bax), but increased the expression of Bcl-2. As is well-known, Bcl-2 and Bax belong to the same family, and they both regulate apoptosis activators by controlling the permeability of mitochondrial membranes. The Bax dimer opens the channel on cell membrane to increase the permeability; while Bcl-2 forms a heteropolymer with Bax, thus reducing the permeability. Increased Bcl-2 levels and decreased Bax suggest that cells are more resistant to apoptosis, which should be the hallmark of protective action, and *vice versa*.

To further explore the possible mechanisms of anti-apoptosis, we embarked on the study of Notch pathway. Notch signaling is an important regulator of cell migration, differentiation, angiogenesis, proliferation and apoptosis, maintaining the intracellular stability [65–69]. It has four receptors (Notch 1–4) and five structurally similar ligands (Delta-like1, Delta-like3, Delta-like4, Jagged-1, Jagged-2) [70,71], of which Notch-1 can be used in a variety of cells. One research has shown that Notch-1 is activated in the early stages of proliferation and differentiation, and down-regulated towards the end of development [72]. Studies by Li et al. [30,73,74] revealed that the expression of Notch-1 is transiently up-regulated in the presence of myocardial injury, suggesting that Notch signaling itself may contribute to cardiac repair. By exogenously stimulating the expression of Notch-1 signaling, the severity of myocardial damage can be improved. The appearance of I/R injury will increase Notch-1 expression, so as to achieve the purpose of self-repair. However, such self-repair is not enough for the damage of the myocardium. In our study, after acupoint gel embedding, the expression of Notch-1 and its ligand (Jagged-1) significantly increases, indicating that acupoint gel embedding might induce cardioprotective effects *via* the Notch-1/Jagged-1 pathway. It is speculated that acupoint gel embedding can activate the Notch signal pathway, improve cardiac function, reduce myocardial fibrosis, shrank the size of infarct, and inhibit cardiomyocyte apoptosis. The in-depth mechanism and the accurate function of the Notch-1/Jagged-1 pathway in the effects of acupoint gel embedding on I/R injury need to be systematically investigated in the future work.

Although in this work we only investigated the protective effects of acupoint gel embedding against myocardial I/R injury in rats, we believe the proposed acupoint gel embedding approach could find wide applications in many disease treatments. More research should be

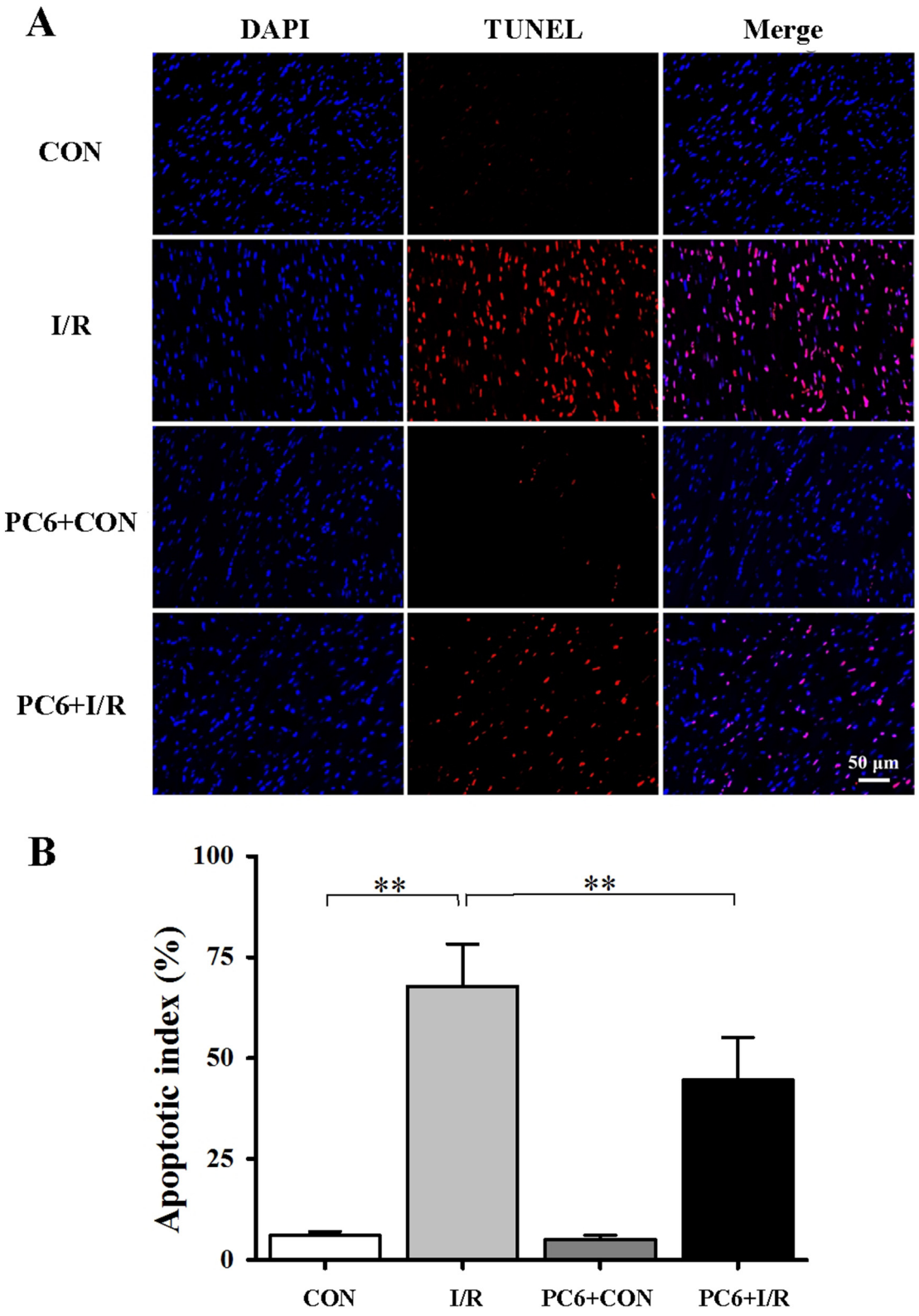


**Fig. 8.** Acupoint gel embedding inhibited cell apoptosis in myocardial tissue. (A) Representative photomicrographs of *in situ* detection of apoptotic myocytes by TUNEL staining. Total nuclei were labeled with DAPI (blue), and apoptotic nuclei were detected by TUNEL staining (red). (B) Quantitative analysis of TUNEL positive cells. The percentage of TUNEL positive cells was expressed as percent DAPI stained cells. Data are shown as mean ± SD, $n = 6$, $^{**}P < 0.01$. (For interpretation of the references to color in this figure legend, the reader is referred to the web version of this article.)

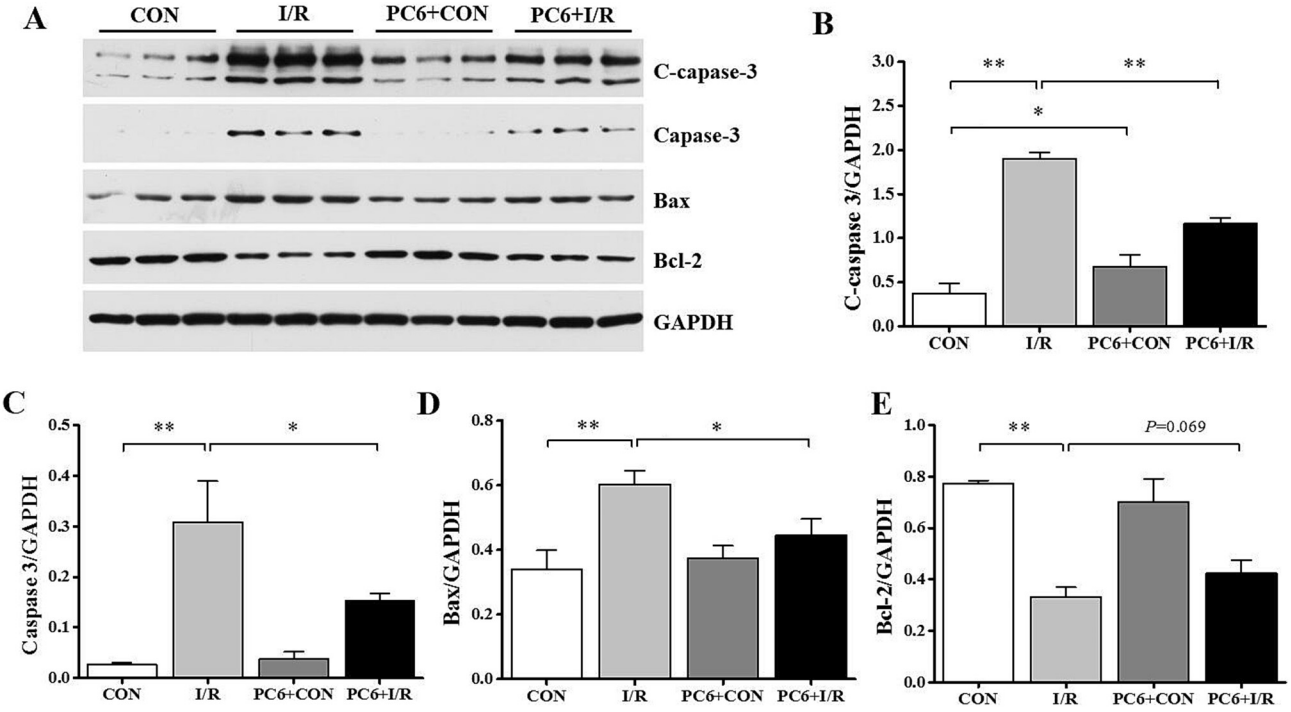


**Fig. 9.** The protein expression of apoptosis-related protein in myocardial Tissue. (A) The protein levels of c-caspase3, caspase-3, Bax and Bcl-2 in myocardial tissues were evaluated by western blotting analysis. Original blots are shown in Supplementary Fig. 4A. (B–E) The expression levels of c-caspase-3, caspase-3, Bax and Bcl-2, respectively. Data are shown as mean ± SD, $n = 3$, $^{*}P < 0.05$, $^{**}P < 0.01$.

performed to optimize acupoint gel embedding to maximize its effectiveness, and to uncover the underlying mechanisms in treating different types of diseases.

## 5. Conclusion

We explored the protective effects of acupoint gel embedding at PC6 points against myocardial I/R injury in rats. Our results showed that acupoint gel embedding could have cardioprotective effects in many

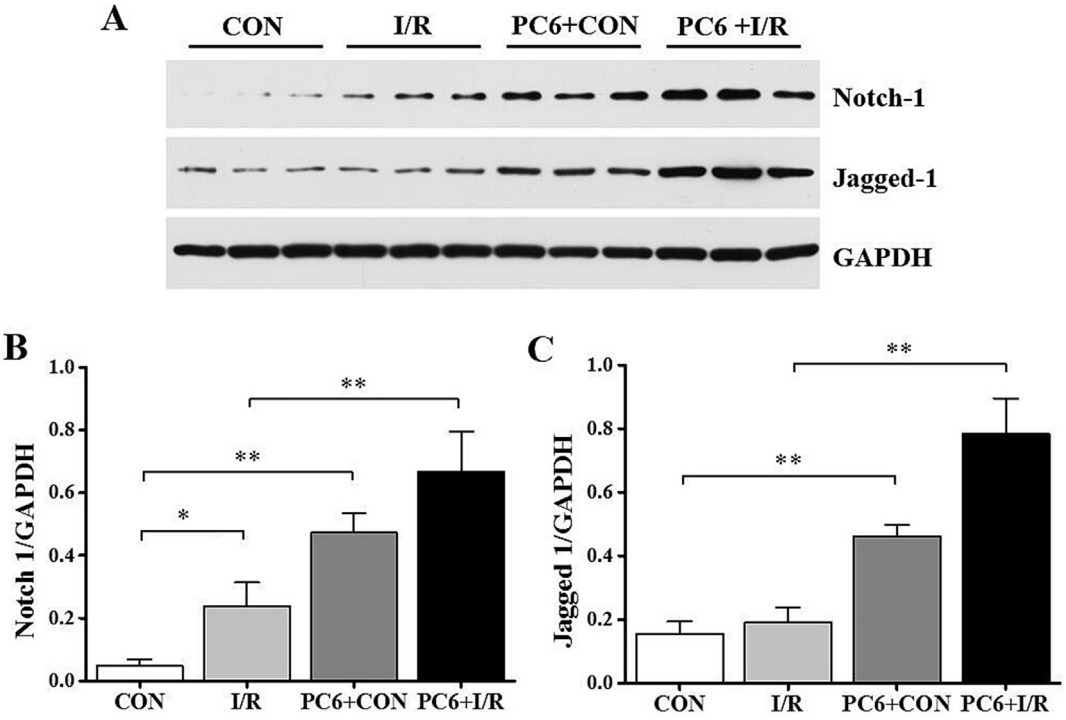


**Fig. 10.** The cardioprotective effect of acupoint gel embedding is associated with enhanced Notch-1 signaling. (A) The protein levels of Notch-1 and Jagged-1 in myocardial tissues were evaluated by western blotting analysis. Original blots are shown in Supplementary Fig. 4B. (B) The expression of Notch-1. (C) The expression of Jagged-1. Data are shown as mean ± SD, $n = 3$, $^{*}P < 0.05$, $^{**}P < 0.01$.

aspects, such as reducing myocardial infarcted size, remitting pathological changes in myocardial tissue, reducing diagnostic marker enzyme activities, attenuating oxidative stress and inflammatory response in I/R hearts, as well as inhibiting cell apoptosis in myocardial tissue. Such cardioprotective effects were found to be associated with Notch-1/Jagged-1 pathway. The developed approach could achieve long-term, well-controlled acupoint stimulation of acupoints with reduced inflammatory response and pain of patient, thus holding great promises in many disease treatments.

Supplementary data to this article can be found online at https://doi.org/10.1016/j.lfs.2018.09.010.

## Acknowledgements

This work was financially supported by the National Natural Science Foundation of China (11522219, 11532009, 11602191, 11872298), the Projects of International (Regional) Cooperation and Exchanges of NSFC (11761161004), the Natural Science Basic Research Plan in Shaanxi Province of China (2016JM8120, 2017JM1026), and the China Postdoctoral Science Foundation (2018M631141).

## Author contributions

C.J., F.S., G.H., T.J.L. and F.X. designed the experiments. C.J., F.S. and H.L. performed the experiments. S.B.L. performed the simulation. C.J., F.S., S.B.L, G.H., T.J.L. and F.X. analyzed the data. All the authors wrote the manuscript. The authors declare no competing financial interests.

## References

[1] J.A. Finegold, P. Asaria, D.P. Francis, Mortality from ischaemic heart disease by country, region, and age: statistics from World Health Organisation and United Nations, Int. J. Cardiol. 168 (2013) 934–945.
[2] D.J. Hausenloy, D.M. Yellon, Targeting myocardial reperfusion injury—the search continues, N. Engl. J. Med. 373 (2015) 1073–1075.
[3] L.M. Buja, R.S. Vander Heide, Pathobiology of ischemic heart disease: past, present and future, Cardiovasc. Pathol. 25 (2016) 214–220.
[4] B. Ibáñez, G. Heusch, M. Ovize, dWF Van, Evolving therapies for myocardial ischemia/reperfusion injury, J. Am. Coll. Cardiol. 65 (2015) 1454.
[5] Y. Zheng, S. Gu, X. Li, J. Tan, S. Liu, Y. Jiang, et al., Berbamine postconditioning protects the heart from ischemia/reperfusion injury through modulation of autophagy, Cell Death Dis. 8 (2017) e2577.
[6] X. Wang, F. He, Y. Liao, X. Song, M. Zhang, L. Qu, et al., Baicalin pretreatment protects against myocardial ischemia/reperfusion injury by inhibiting mitochondrial damage-mediated apoptosis, Int. J. Cardiol. 168 (2013) 4343.
[7] S.F. Lu, Y. Huang, N. Wang, W.X. Shen, S.P. Fu, Q. Li, et al., Cardioprotective effect of electroacupuncture pretreatment on myocardial ischemia/reperfusion injury via antiapoptotic signaling, Evid. Based Complement. Alternat. Med. (2016) 4609784.
[8] P.-P. Hao, F. Jiang, Y.-G. Chen, J. Yang, K. Zhang, M.-X. Zhang, et al., Traditional Chinese medication for cardiovascular disease, Nat. Rev. Cardiol. 12 (2015) 115–122.
[9] Cheng TO, Acupuncture in Cardiology, INTECH Open Access Publisher, 2013.
[10] S.S. Chavan, K.J. Tracey, Regulating innate immunity with dopamine and electroacupuncture, Nat. Med. 20 (2014) 239–241.
[11] Z. Liu, Y. Liu, H. Xu, L. He, Y. Chen, L. Fu, et al., Effect of electroacupuncture on urinary leakage among women with stress urinary incontinence: a randomized clinical trial, JAMA 317 (2017) 2493.
[12] R. Torres-Rosas, G. Yehia, G. Pena, P. Mishra, M.D. Thompson-Bonilla, M.A. Moreno-Eutimio, et al., Dopamine mediates vagal modulation of the immune system by electroacupuncture, Nat. Med. 20 (2014) 291–295.
[13] N. Goldman, M. Chen, T. Fujita, Q.W. Xu, W.G. Peng, W. Liu, et al., Adenosine A1 receptors mediate local anti-nociceptive effects of acupuncture, Nat. Neurosci. 13 (2010) (883-U130).
[14] W.S. Sun, Micro-invasive thread embedding: a new approach for acupuncture medicine, J. Integr. Med. 12 (2014) 249.
[15] C. Nardini, S. Carrara, Y.H. Liu, V. Devescovi, Y.T. Lu, X.Y. Zhou, i-Needle: detecting the biological mechanisms of acupuncture, Science 346 (2014) S21–S22.
[16] S.L. In, Y.S. Gwak, H.R. Kim, A. Razzaq, K.S. Lee, H.Y. Kim, et al., Hierarchical micro/nano-porous acupuncture needles offering enhanced therapeutic properties, Sci. Rep. 6 (2016).
[17] Y.X. Xu, J.Y. Cai, L.Q. Liang, G.Z. Chen, X.L. Xu, The application of nanotechnology in acupoint catgut embedding therapy, Mater. Sci. Forum (2011) 68–72.
[18] L. Jia, X. Tong, L. Jiayu, Z. Siyu, W. Tong, S. Shiyao, et al., Adverse reactions of acupoint embedding and its treatment, Chin. Acupunct. Moxibustion 36 (2016) 1166–1168.
[19] X. Tong, F. Yang, Recent progress in developing injectable materials for enhancing cell delivery and tissue regeneration, Adv. Healthcare Mater. 7 (2018) 1701065.
[20] T.D. Johnson, K.L. Christman, Injectable hydrogel therapies and their delivery strategies for treating myocardial infarction, Expert Opin. Drug Deliv. 10 (2013) 59–72.
[21] A. Hasan, A. Khattab, M.A. Islam, K.A. Hweij, J. Zeitouny, R. Waters, et al., Injectable hydrogels for cardiac tissue repair after myocardial infarction, Adv. Sci. 2 (2015) 1–18.
[22] G. Huang, F. Li, X. Zhao, Y. Ma, Y. Li, M. Lin, et al., Functional and biomimetic materials for engineering of the three-dimensional cell microenvironment, Chem. Rev. 117 (2017) 12764–12850.
[23] M.C. Serrano, E.J. Chung, G.A. Ameer, Advances and applications of biodegradable elastomers in regenerative medicine, Adv. Funct. Mater. 20 (2010) 192–208.
[24] H.K. Makadia, S.J. Siegel, Poly lactic-co-glycolic acid (PLGA) as biodegradable controlled drug delivery carrier, Polymer 3 (2011) 1377.
[25] W. Ying, W.S. Zhao, D. Li, Y.H. Xu, M.D. Li, J. Chen, et al., The beneficial effects of electroacupuncture at PC6 acupoints (Neiguan) on myocardial ischemia in ASIC3 −/− mice, J. Acupunct. Meridian Stud. 11 (2018) 88–96.
[26] Y. Wang, W. Wang, D. Li, J. Li, J. Dai, Y. Liu, et al., The beneficial effect of electroacupuncture given at PC6 (Neiguan-point) by the increase in cardiac transient outward K+ current channel which depends on the gene and protein expressions in artificially induced myocardial ischemia rats, Acupunct. Electrother. Res. 39 (2014) 259–273.
[27] L. Shi, J. Fang, J. Zhao, G. Liu, Q. Zhao, J. Zhang, et al., Comparison of the therapeutic effects of acupuncture at PC6 and ST36 for chronic myocardial ischemia, Evid. Based Complement. Alternat. Med. (2017) 2017 (7358059).
[28] L. Liu, S. Wang, C. Fu, S. Shu, M. Fu, J. Li, et al., Comparison of beneficial effects of acupuncture at PC6, LU7 & non-acupuncture points on cardiac cell function in myocardial ischemia (MI) rats by testing protein expression of L-type calcium channel protein and its related protein, Acupunct. Electrother. Res. 41 (2016) 107–125.
[29] H. Zhu, X. Wang, M. Huang, Y. Jing, D. Zhang, G. Ding, Mast cell activation in the acupoint is important for the electroacupuncture effect against pituitrin-induced bradycardia in rabbits, Sci. Rep. 7 (2017) 9040.
[30] L. Yu, Y. Sun, L. Cheng, Z. Jin, Y. Yang, M. Zhai, et al., Melatonin receptor-mediated protection against myocardial ischemia/reperfusion injury: role of SIRT1, J. Pineal Res. 57 (2014) 228–238.
[31] S. Korkmaz, E. Barnucz, S. Loganathan, S. Li, T. Radovits, P. Hegedus, et al., Q50, an iron-chelating and zinc-complexing agent, improves cardiac function in rat models of ischemia/reperfusion-induced myocardial injury, Circ. J. 77 (2013) 1817.
[32] F. Song, F. Hua, H. Li, X.X. Zhou, L. Yan, Q. Yang, et al., Cardiac stem cell transplantation with 2,3,5,4′-tetrahydroxystilbehe-2-O-beta-D-glucoside improves cardiac function in rat myocardial infarction model, Life Sci. 158 (2016) 37–45.
[33] L. Hua, S. Fan, L.R. Duan, J.J. Sheng, Y.H. Xie, Y. Qian, et al., Paeonol and danshensu combination attenuates apoptosis in myocardial infarcted rats by inhibiting oxidative stress: roles of Nrf2/HO-1 and PI3K/Akt pathway, Sci. Rep. 6 (2016) 23693.
[34] P.C. Westman, M.J. Lipinski, D. Luger, R. Waksman, R.O. Bonow, E. Wu, et al., Inflammation as a driver of adverse left ventricular remodeling after acute myocardial infarction, J. Am. Coll. Cardiol. 67 (2016) 2050–2060.
[35] Z. Li, Clinical observation in 46 cases of angina pectoris treated by the catgut-embedding therapy, J. Tradit. Chin. Med. 23 (2003) 199–200.
[36] W. Qin, K. Zhao, H. Yang, Effect of acupoint catgut embedding therapy combined with Chinese medicine for nourishing the kidneys and promoting blood circulation and improving blood glucose and lipid levels as well as the pregnancy rate in obese PCOS patients with infertility, Exp. Ther. Med. 12 (2016) 2909–2914.
[37] Y. Sun, L. Ye, C. Jiang, J. Jiang, H. Hong, L. Qiu, Over-expression of HSPA12B protects mice against myocardium ischemic/reperfusion injury through a PPARgamma-dependent PI3K/Akt/eNOS pathway, Am. J. Transl. Res. 7 (2015) 2724–2737.
[38] H. Zhu, A. Sun, Programmed necrosis in heart disease: molecular mechanisms and clinical implications, J. Mol. Cell. Cardiol. (2018), https://doi.org/10.1016/j.yjmcc.2018.01.018.
[39] J. Wu, J.G. Hecker, N. Chiamvimonvat, Antioxidant enzyme gene transfer for ischemic diseases, Adv. Drug Deliv. Rev. 61 (2009) 351–363.
[40] T.N. Andrienko, P. Pasdois, G.C. Pereira, M.J. Ovens, A.P. Halestrap, The role of succinate and ROS in reperfusion injury – a critical appraisal, J. Mol. Cell. Cardiol. 110 (2017) 1–14.
[41] G. Barrera, S. Pizzimenti, M. Daga, C. Dianzani, A. Arcaro, G.P. Cetrangolo, et al., Lipid peroxidation-derived aldehydes, 4-hydroxynonenal and malondialdehyde in aging-related disorders, Antioxidants 7 (2018).
[42] Y.T. Li, L.N. Tang, Y. Ning, Q. Shu, F.X. Liang, H. Wang, et al., In vivo monitoring of serotonin by nanomaterial functionalized acupuncture needle, Sci. Rep. 6 (2016).
[43] L.N. Tang, D.X. Du, F. Yang, Z. Liang, Y. Ning, H. Wang, et al., Preparation of graphene-modified acupuncture needle and its application in detecting neurotransmitters, Sci. Rep. 5 (2015).
[44] C. Wang, X. Wang, K. Dong, J. Luo, Q. Zhang, Y. Cheng, Injectable and responsively degradable hydrogel for personalized photothermal therapy, Biomaterials 104 (2016) 129–137.
[45] J.-A. Yang, J. Yeom, B.W. Hwang, A.S. Hoffman, S.K. Hahn, In situ-forming injectable hydrogels for regenerative medicine, Prog. Polym. Sci. 39 (2014) 1973–1986.
[46] Y. Li, G. Huang, M. Li, L. Wang, E.L. Elson, T.J. Lu, et al., An approach to quantifying 3D responses of cells to extreme strain, Sci. Rep. 6 (2016) 19550.
[47] Y. Li, G. Huang, B. Gao, M. Li, G.M. Genin, T.J. Lu, et al., Magnetically actuated cell-laden microscale hydrogels for probing strain-induced cell responses in three

dimensions, NPG Asia Mater. 8 (2016) e238.
[48] C.A. Cezar, E.T. Roche, H.H. Vandenburgh, G.N. Duda, C.J. Walsh, D.J. Mooney, Biologic-free mechanically induced muscle regeneration, Proc. Natl. Acad. Sci. U. S. A. 113 (2016) 1534–1539.
[49] H.S. O'Neill, L.B. Gallagher, J. O'Sullivan, W. Whyte, C. Curley, E. Dolan, et al., Biomaterial-enhanced cell and drug delivery: lessons learned in the cardiac field and future perspectives, Adv. Mater. 28 (2016) 5648–5661.
[50] M. Amani, S. Jeddi, N. Ahmadiasl, N. Usefzade, J. Zaman, Effect of HEMADO on level of CK-MB and LDH enzymes after ischemia/reperfusion injury in isolated rat heart, BioImpacts 3 (2013) 101–104.
[51] M. Neri, S. Bello, A. Bonsignore, F. Centini, C. Fiore, Z. Foldes-Papp, et al., Myocardial expression of TNF-alpha, IL-1beta, IL-6, IL-8, IL-10 and MCP-1 after a single MDMA dose administered in a rat model, Curr. Pharm. Biotechnol. 11 (2010) 413–420.
[52] H. Pei, X. Song, C. Peng, Y. Tan, Y. Li, X. Li, et al., TNF-alpha inhibitor protects against myocardial ischemia/reperfusion injury via Notch1-mediated suppression of oxidative/nitrative stress, Free Radic. Biol. Med. 82 (2015) 114–121.
[53] J. Li, H. Zhang, C. Zhang, Role of inflammation in the regulation of coronary blood flow in ischemia and reperfusion: mechanisms and therapeutic implications, J. Mol. Cell. Cardiol. 52 (2012) 865–872.
[54] N.L. Lohr, A. Keszler, P. Pratt, M. Bienengraber, D.C. Warltier, N. Hogg, Enhancement of nitric oxide release from nitrosyl hemoglobin and nitrosyl myoglobin by red/near infrared radiation: potential role in cardioprotection, J. Mol. Cell. Cardiol. 47 (2009) 256–263.
[55] C. Farah, A. Nascimento, G. Bolea, G. Meyer, S. Gayrard, A. Lacampagne, et al., Key role of endothelium in the eNOS-dependent cardioprotection with exercise training, J. Mol. Cell. Cardiol. 102 (2017) 26–30.
[56] S.D. Prabhu, N.G. Frangogiannis, The biological basis for cardiac repair after myocardial infarction: from inflammation to fibrosis, Circ. Res. 119 (2016) 91–112.
[57] M.F. Yuyun, L.L. Ng, G.A. Ng, Endothelial dysfunction, endothelial nitric oxide bioavailability, tetrahydrobiopterin, and 5-methyltetrahydrofolate in cardiovascular disease. Where are we with therapy? Microvasc. Res. 119 (2018) 7–12.
[58] F.X. Yan, H.M. Li, S.X. Li, S.H. He, W.P. Dai, Y. Li, et al., The oxidized phospholipid POVPC impairs endothelial function and vasodilation via uncoupling endothelial nitric oxide synthase, J. Mol. Cell. Cardiol. 112 (2017) 40–48.
[59] F. Santilli, D. D'Ardes, G. Davi, Oxidative stress in chronic vascular disease: from prediction to prevention, Vasc. Pharmacol. 74 (2015) 23–37.
[60] H.N. Siti, Y. Kamisah, J. Kamsiah, The role of oxidative stress, antioxidants and vascular inflammation in cardiovascular disease (a review), Vasc. Pharmacol. 71 (2015) 40–56.
[61] A. Lejay, F. Fang, R. John, J.A.D. Van, M. Barr, F. Thaveau, et al., Ischemia reperfusion injury, ischemic conditioning and diabetes mellitus, J. Mol. Cell. Cardiol. 91 (2016) 11–22.
[62] M. Neri, V. Fineschi, M. Di Paolo, C. Pomara, I. Riezzo, E. Turillazzi, et al., Cardiac oxidative stress and inflammatory cytokines response after myocardial infarction, Curr. Vasc. Pharmacol. 13 (2015) 26–36.
[63] S. Ghaderi, N. Alidadiani, N. Dilaver, H.R. Heidari, R. Parvizi, R. Rahbarghazi, et al., Role of glycogen synthase kinase following myocardial infarction and ischemia-reperfusion, Apoptosis 22 (2017) 887–897.
[64] L.P. Zhu, T.T. Wei, J. Gao, X.Y. Chang, H. He, F. Luo, et al., The cardioprotective effect of salidroside against myocardial ischemia reperfusion injury in rats by inhibiting apoptosis and inflammation, Apoptosis 20 (2015) 1433–1443.
[65] X.L. Zhou, R.R. Zhu, S. Liu, H. Xu, X. Xu, Q.C. Wu, et al., Notch signaling promotes angiogenesis and improves cardiac function after myocardial infarction, J. Cell. Biochem. 119 (2018) 7105–7112.
[66] Y. Li, Y. Hiroi, J.K. Liao, Notch signaling as an important mediator of cardiac repair and regeneration after myocardial infarction, Trends Cardiovasc. Med. 20 (2010) 228–231.
[67] H. Pei, Q. Yu, Q. Xue, Y. Guo, L. Sun, Z. Hong, et al., Notch1 cardioprotection in myocardial ischemia/reperfusion involves reduction of oxidative/nitrative stress, Basic Res. Cardiol. 108 (2013) 373.
[68] N. Gude, M. Sussman, Notch signaling and cardiac repair, J. Mol. Cell. Cardiol. 52 (2012) 1226–1232.
[69] H. Gong, Y. Yan, B. Fang, Y.Y. Xue, P.P. Yin, L. Li, et al., Knockdown of nucleosome assembly protein 1-like 1 induces mesoderm formation and cardiomyogenesis via Notch signaling in murine-induced pluripotent stem cells, Stem Cells 32 (2014) 1759–1773.
[70] F. Wu, B. Yu, X. Zhang, Y. Zhang, Cardioprotective effect of Notch signaling on the development of myocardial infarction complicated by diabetes mellitus, Exp. Ther. Med. 14 (2017) 3447–3454.
[71] S. Rentschler, A.H. Yen, J. Lu, N.B. Petrenko, M.M. Lu, L.J. Manderfield, et al., Myocardial Notch signaling reprograms cardiomyocytes to a conduction-like phenotype, Circulation 126 (2012) 1058–1066.
[72] I. Cortegano, P. Melgar-Rojas, L. Luna-Zurita, M. Siguero-Alvarez, M.A. Marcos, M.L. Gaspar, et al., Notch1 regulates progenitor cell proliferation and differentiation during mouse yolk sac hematopoiesis, Cell Death Differ. 21 (2014) 1081–1094.
[73] Y. Li, Y. Hiroi, S. Ngoy, R. Okamoto, K. Noma, C.Y. Wang, et al., Notch1 in bone marrow-derived cells mediates cardiac repair after myocardial infarction, Circulation 123 (2011) 866–876.
[74] M. Zhang, L.M. Yu, H. Zhao, X.X. Zhou, Q. Yang, F. Song, et al., 2,3,5,4'-Tetrahydroxystilbene-2-O-beta-D-glucoside protects murine hearts against ischemia/reperfusion injury by activating Notch1/Hes1 signaling and attenuating endoplasmic reticulum stress, Acta Pharmacol. Sin. 38 (2017) 317–330.